12-1-2017

Three-Dimensional Vapor Intrusion Modeling Approach that Combines Wind and Stack Effects on Indoor, Atmospheric, and Subsurface Domains

Elham Shirazi
University of Kentucky, elham.shirazi@uky.edu

Kelly G. Pennell
University of Kentucky, kellypennell@uky.edu

Digital Object Identifier (DOI)
https://doi.org/10.1039/C7EM00423K

HHS Public Access

Author manuscript

Environ Sci Process Impacts. Author manuscript; available in PMC 2018 December 13.

Published in final edited form as:

Environ Sci Process Impacts. 2017 December 13; 19(12): 1594–1607. doi:10.1039/c7em00423k.

Three-Dimensional Vapor Intrusion Modeling Approach that Combines Wind and Stack Effects on Indoor, Atmospheric, and Subsurface Domains

Elham Shirazi[a] and **Kelly G. Pennell**[a,*]

[a]University of Kentucky, Department of Civil Engineering, Lexington, KY 40506, USA

Abstract

Vapor intrusion exposure risks are difficult to characterize due to the role of atmospheric, building and subsurface processes. This study presents a three-dimensional VI model that extends the common subsurface fate and transport equations to incorporate wind and stack effects on indoor air pressure, building air exchange rate (AER) and indoor contaminant concentration to improve VI exposure risk estimates. The model incorporates three modeling programs: 1) COMSOL Multiphysics to model subsurface fate and transport processes, 2) CFD0 to model atmospheric air flow around the building, and 3) CONTAM to model indoor air quality. The combined VI model predicts AER values, zonal indoor air pressures and zonal indoor air contaminant concentrations as a function of wind speed, wind direction and outdoor and indoor temperature. Steady state modeling results for a single-story building with a basement demonstrate that wind speed, wind direction and opening locations in a building play important roles in changing the AER, indoor air pressure, and indoor air contaminant concentration. Calculated indoor air pressures ranged from approximately −10Pa to +4Pa depending on weather conditions and building characteristics. AER values, mass entry rates and indoor air concentrations vary depending on weather conditions and building characteristics. The presented modeling approach can be used to investigate the relationship between building features, AER, building pressures, soil gas concentrations, indoor air concentrations and VI exposure risks.

INTRODUCTION

Vapor intrusion (VI) is a process by which volatile organic compounds (VOCs) migrate through the soil from a subsurface vapor source into the indoor air of nearby buildings. Exposure risks related to VI have been a growing concern in recent years and the United States Environmental Protection Agency (USEPA) recently established VI guidance.[1] While indoor air targets exist for many contaminants of concern at VI sites, regulatory standards do not currently exist for soil vapor concentrations. Therefore, USEPA recommends non-traditional data sets (i.e. multiple lines of evidence) to evaluate the potential for VI exposure risks.[1] The multiple lines of evidence approach provides a flexible framework for

*Corresponding Author: kellypennell@uky.edu, Phone: +1 (859) 218-2540, Fax: +1 (859) 257-4404.

Conflicts of interest: The authors have declared no conflict of interest.

investigating vapor intrusion; however, there is a need to improve the understanding of how building operation and atmospheric conditions affect VI exposure risks.

Professional judgement and inclusion of multiple lines of evidence when conducting VI site assessments is widely acknowledged as valuable.[1] Since no other published VI modeling approach has attempted to predict AERs or indoor air concentrations based on weather conditions or specific building features, the model presented here is meant to help inform about processes that are not yet well understood within the VI community. The number of field studies to compare the results of VI models is small, and practically speaking, model verification using field data is not currently feasible and presently there is no VI model that has been fully validated in the field. However, it is important that new models are compared to previously well-established modeling approaches. The results of the model developed as part of this research was compared to two previously published models[2, 3] for select cases. In addition, the model was qualitatively compared to field data from Lou et al.[4]

Over the past several years, many VI models have been developed to predict VI exposure risks[2–20] and none of these models have been fully field validated, but they remain valuable to the VI community in helping to theorectically describe complex VI processes. With few exceptions, VI models are commonly employed as screening tools. Screening models provide information about whether additional site investigation is warranted. A widely employed screening tool is based on the efforts of Johnson and Ettinger.[11] This model (known as the Johnson and Ettinger, or J&E model) is a one-dimensional (1-D) approximation, and has been adapted as a spreadsheet program by several regulatory agencies for risk-based screening purposes (e.g. USEPA[10]). More recently, USEPA has developed a screening level calculator that relies on empirically-based data to establish screening levels for VOCs at VI sites.[21] The screening VI models primarily focus on soil gas entry, with little emphasis on complex role aboveground processes play in the VI process.

The emergence of three-dimensional (3-D) vapor intrusion models has provided considerable insight into the VI process and are an important tool within the multiple lines of evidence framework for assessing vapor intrusion exposure risks.[13] One of the first 3-D VI models incorporated a finite difference numerical code in which a continuity equation was coupled with a chemical transport equation to calculate the soil gas pressure, velocity and chemical concentration in soil and indoor air.[2, 5, 7] Later, Pennell et al.[3] developed a similar 3-D VI model, but incorporated a commercially-available finite element numerical code.[3] Most 3-D VI models have focused on subsurface transport process; however only a few have considered aboveground processes (e.g. Luo et al.[4]).

Reichman et al.[22] reviewed the importance of considering building air exchange rates (AERs) when evaluating VI exposure risks; and, other VI researchers have also highlighted the role that factors such as wind flow and temperature can have on contaminant transport in subsurface and also indoor air concentration distribution.[4, 12, 14, 15, 18, 19] Reichman et al.[22] noted that existing VI models require users to input generic building pressures and AERs even though indoor air science research provides tools to determine AERs and building pressures based on building characteristics, occupant behavior and weather conditions.

In this study, we improve existing VI models by incorporating wind and stack effects, and building characteristics to calculate indoor air pressures, AERs, and indoor air concentrations. We present a theoretical basis, overall governing equations, a general modeling approach that combines subsurface VI model approaches with a multizone indoor air quality model coupled with an outdoor atmospheric model and provide illustrative results.

THEORY AND METHODS

This manuscript presents a framework for a new modeling approach that advances current VI models by linking existing subsurface VI models to an aboveground computational fluid dynamic (CFD) program and a multizone indoor air quality modeling program. Multizone indoor air quality programs predict infiltration and exfiltration through openings of different building zones under given weather conditions.[23, 24] These programs are especially valuable because they can calculate the airflow and relative pressures between different building zones and AER values.[25, 26] They have been used for indoor air quality, including radon intrusion studies.[27] Recently multizone programs have been improved by coupling with CFD programs to combine the effect of indoor and outdoor air quality on pressure gradients and air flow rate distribution in a building.[28, 29]

Background

AERs are known as an important parameter that control indoor air quality. Weather condition and building condition and operation (air conditioning status and occupant preference) are factors that can affect AERs. Recently, Reichman et al.[22] reviewed several indoor air quality studies and highlighted important considerations for including accurate estimates of AERs during VI assessments. In addition, they summarized methods for estimating AERs.

Wind and stack effects are two driving forces that influence AER, indoor-outdoor pressure differences, and consequently VI exposure risks. Stack effect is caused by air density differences that result from temperature differences between indoor and outdoor air. Wind flow not only influences AER and air pressure inside a building, but also influences the ground surface pressure adjacent to the building, which consequently alters the soil gas flow and subsurface soil gas concentrations under the building.[12, 14, 15] Previous radon research has highlighted the importance of wind and stack effects for radon intrusion. For instance, Riley et al.[14, 15] used the mean ground-surface pressure coefficients obtained from a wind tunnel experiment on a single family structure to investigate the effect of wind speed and direction on radon concentration in soil and indoor air.[14, 15] While Riley et al.[14, 15] models did not account for stack effect on indoor air pressure, Sherman[30] stated that stack effect is more effective than wind effect in changing the radon entry rate into a building.

A few vapor intrusion models have specifically investigated the role of stack and wind effects. Song et al.[19] assessed the influence of stack and wind effects on soil gas entry rate and outdoor air flowrate through the building, however the authors did not consider wind effect (or wind direction) on subsurface pressure, which influences on soil gas entry rate.[19] Shen and Suuberg[18] showed that the AER and indoor air pressure variation can result in

substantial variation in indoor air contaminant concentration; however they did not indicate how wind and temperature influence AER or indoor air pressure.[18] Although these studies are important in highlighting the importance of aboveground processes on VI, these studies have not considered how AER and indoor air pressure are directly connected to wind and stack effects, and how together all of these parameters collectively alter VI exposure risks.

To date, one of the most comprehensive VI studies to investigate wind and stack effects involved a site in Evansville, Wyoming.[4, 12] The findings showed that wind flow is important in influencing (an aerobically biodegradable) contaminant and oxygen concentrations in the soil under a building. The results showed low concentration of contaminant and high concentration of oxygen at the windward side of the building, while a high concentration of contaminant and depleted oxygen was reported on the leeward side of the building.[4, 12] The study concluded that the oxygen delivered to the soil by wind on the windward side enhanced aerobic biodegradation of the contaminant. Luo[12] developed a numerical model that modified the 3-D VI model previously developed by Abreu and Johnson[2] to account for the influence of wind and stack effects; however the modified model did not consider the effect of wind and stack effects on AER when calculating the indoor air concentration.[12]

The research described herein presents a modeling framework that advances previous modeling efforts by accounting for the influence of wind and stack effects on AER, indoor-outdoor pressure differences, ground surface pressures, and predicts indoor air contaminant concentrations using a multizone model.

Model Method

This study relies on three modeling programs: 1) a three dimensional finite element Multiphysics program known as COMSOL Multiphysics, 2) CFD0 which is a CFD program, and 3) CONTAM which is a multizone indoor air quality and ventilation analysis computer program developed by the Building and Fire Research Laboratory of the National Institute of Standards and Technology (NIST). CFD0 and CONTAM are both freely available software through the Building and Fire Research Laboratory of NIST.

In VI studies, most existing VI models incorporate a user defined value for indoor air pressure as a boundary condition; however, indoor air pressure is influenced by wind and stack effect.[31] To investigate wind and stack effects, this research uses an indirect coupling approach between CONTAM and CFD0 through the air flowrates at the interfaces. Indirect coupling used by Wang[28] is a one-step strategy in which CFD0 and CONTAM run sequentially.

CONTAM runs two times in this study: One time to calculate basement pressure and AER (CONTAM (1)). The basement pressure is used as boundary condition in COMSOL; and one time to calculate indoor air contaminant concentration (CONTAM (2)) after the mass entry rate of contaminant through the cracks is obtained by COMSOL. Figure 1 illustrates a step by step overview of the modeling process used in the present study. In Step 1, the user inputs the building characteristics and the wind direction range (0–360°). CFD0 solves the Reynolds Averaged Navier-Stokes (RANS) equations to calculate the distribution of wind

pressure on building surface. Then, CFD0 converts the wind pressures on the building envelope to wind pressure coefficients (C_p) using Bernoulli's equation (Step 1, Figure 1).[29]

In step 2(a) and 2(b) (Figure 1), C_p values are assigned to each flow path (any small or large opening) of the building for variable wind directions in wind pressure profile (WPP). Small openings around windows, doors, or walls can be considered as small flow paths, and open window and doors can be considered as large flow paths. The user defines the path locations in Step 2a which depends on building characteristics. CONTAM (1) calculates the AER, the zonal indoor air pressures and air mass flowrates through the paths by solving the mass balance equations for all the zones considering wind effect (by C_p values) and stack effect (Step 3, Figure 1).[29]

In step 4, zonal pressures obtained in step 3 are used as boundary conditions for foundation cracks in COMSOL. Unlike previous VI models (e.g. Pennell et al.[3]), where the pressure at the foundation cracks were defined by the user, in this model, the boundary condition at the crack is defined by the results from CONTAM (1) and is influenced by stack and wind effects. The influence of wind flows on the pressure outside of the building in the surrounding air and soil domains, as well as the contaminant concentration in soil domain, is determined by COMSOL. COMSOL calculates the mass entry rate of contaminant near the foundation cracks which is used as inputs in step 5 (Figure 1). In step 5, CONTAM (2) calculates the indoor air concentration of contaminant considering the zonal pressures, infiltration and exfiltration rates and AER obtained in step 3. Both COMSOL and CFD0 solve for the wind pressure. COMSOL solves for the wind pressure in atmospheric air and on the ground surface. COMSOL links the ground surface pressure created by wind to the subsurface soil pressure to investigate how wind flow influences subsurface soil pressure and consequently soil gas concentration. CFD0 is used to calculate the pressure coefficients on the building surface. CFD0 is then coupled to CONTAM to calculate indoor pressure and building AER based on wind and stack effects. The COMSOL and CFD0 wind pressure results in the atmospheric domain are compared to ensure agreement between modeling approaches.

Turbulent (wind) flows are solved using a segregated approach to prevent the solution from becoming ill-conditioned. Each iteration of the RANS group involves a sub-iteration of two or three repetitions conducted for the turbulence transport equations. Specifically, the sub-iteration is required to assure the balance of the very non-linear source term in the turbulence transport equations before the next iteration for the RANS group. The default iterative solver for the turbulence transport equations in COMSOL is GMRES accelerated by Geometric Multigrid.

The overall governing equations used in this modeling process are as follows:

CONTAM calculates indoor air pressure by solving mass balance equations for all the zones.[32] In a steady state condition the principle of conservation of mass states that:

$$\sum_j F_{ji} = 0 \quad (1$$

where F_{ji} (kg/s) is the air mass flow rate between zones j and i which is a function of the pressure drop between these two zones. A positive value for F_{ji} shows that air is flowing from zone j to zone i and a negative value indicates an opposite direction from i to j.

In this study, CONTAM calculates the air mass flow rate (F_{ji}) through a crack or opening in a building envelope based on the power law equation for different types of air flow paths:

$$F_{ji}=C(\Delta P)^n \quad (2$$

where ΔP (Pa) is the pressure difference across a flow path between zones j and i, C (kg/s.Pa^n) is the flow coefficient, and n (dimensionless) is the flow exponent which, theoretically, lies between 0.5 and 1 values. Orme et al.[33] showed that n varies between 0.6 and 0.7 in houses. In this study we use 0.65 for n value (for closed windows, doors and external walls) which is a typical value for small crack-like openings. For cracks, CONTAM uses equation 3:[32]

$$n=0.5+0.5\exp(-\frac{W}{2}) \quad (3$$

In which W is the crack width in mm.

Using equation 4, CONTAM converts the parameters that describe an opening to flow coefficient (C) in equation 2:

$$C=LC_d\sqrt{2}(\Delta P_r)^{\frac{1}{2}-n} \quad (4$$

where C_d (dimensionless) is the discharge coefficient, ΔP_r (Pa) is the reference pressure difference on a pressurization test. The set of reference condition used in this study is C_d =1 and ΔP_r = 4 Pa. L (cm^2/m^2 or cm^2 per item) is the effective leakage area of an opening in the building. Typical leakage areas for residential buildings have been provided in chapter 26 of 2001 ASHRAE Handbook of Fundamentals (see table 1 of ASHRAE[34]).

In equation 2, pressure difference between two zones (ΔP) for each air flow path is calculated using equation 5 which includes three components: 1) wind effect, 2) stack effect, and 3) zone pressure difference.

$$\Delta P=P_j-P_i+P_s+P_w \quad (5$$

where P_j (Pa) and P_i (Pa) are total pressure at zones j and i, respectively. P_s (Pa) is the pressure difference due to stack effect and P_w (Pa) is the pressure difference induced by wind effect. Pressure difference caused by stack and wind effect at height H is computed

using the equations 6 and 7, respectively, based on 2013 ASHRAE Handbook of Fundamentals.[31]

$$P_s = \rho g (H_{NPL} - H) \left(\frac{T_{in} - T_{out}}{T_{in}} \right) \quad (6$$

where ρ (kg/m^3) is outdoor air density, g (m/s^2) is gravitational acceleration, H_{NPL} (m) is the location in the building envelope where there is no indoor-to-outdoor pressure difference, and T_{in} (°C) and T_{out} (°C) are the indoor and outdoor temperatures, respectively.

$$P_w = \frac{1}{2} \rho U_H^2 C_p \quad (7$$

where U_H (m/s) is the wind velocity at the reference height H (m) that can be calculated as follows:

$$U_H = U_{met} \left(\frac{\delta_{met}}{H_{met}} \right)^{\alpha_{met}} \left(\frac{H}{\delta} \right)^{\alpha} \quad (8$$

In which, U_{met} (m/s) is the wind velocity at the height of H_{met} (m); H_{met} is the reference height at the meteorological station (Usually 10m above ground level); δ_{met} (m) and α_{met} (dimensionless) are the atmospheric boundary layer thickness and the exponent at meteorological station, respectively. δ (m) and α (dimensionless) are the corresponding values for the local building terrain which can be found in chapter 24 of 2013 ASHRAE Handbook of Fundamentals (see table 1 of ASHRAE[31]).

To calculate C_p (the wind pressure coefficient for the airflow path), CONTAM is coupled with a CFD program (CFD0) through the airflow rates or pressure drops at the interfaces. CFD0 solves the Reynolds Averaged Navier-Stokes equations to calculate the distribution of wind pressure on building surface. Then wind pressure coefficients will be calculated using Bernoulli's equation (Equation 9):

$$C_P = \frac{P_D}{\frac{1}{2} \rho U_H^2} \quad (9$$

where C_P (dimensionless) is the wind pressure coefficient at a point on the building surface, P_D (Pa) is the difference between wind pressure on the building surface and the free-stream pressure. C_p values will be calculated by CFD0 for a specific local terrain feature and different wind directions. C_p values are a function of location of the paths on a building surface and wind direction. Wang et al.[29] compared the predicted wind pressure coefficients (using CFD0) with measured data[35, 36] and the results showed that the calculated values are in good agreement with measured data.

Based on the equations above, equation 1 is a nonlinear function of P_i and P_j:

$$\sum_j F_{ji} = \sum_j f(P_j, P_i) = 0 \quad (10$$

Regarding equation 10, the steady state mass flow analysis for multiple zones requires the simultaneous solution of nonlinear equations by Newton-Raphson method until a convergent solution of the set of zone pressures is attained (P_j, P_i, …, P_n).

Zones can be defined in CONTAM with either known or unknown pressures. Unknown pressure zones are linked by pressure dependent flow paths to a constant pressure zone, like an ambient zone (when there is no wind flow the ambient pressure would be equal to zero and in case wind is blowing, ambient pressure will be calculated using CFD0).

Once the zonal pressures are computed, the air mass flow rates are calculated using equation 2. Contaminant concentration in each zone then can be calculated based on conservation of mass in each zone. CONTAM uses the following conservation of mass equation in steady state condition to compute the contaminant concentration in each zone[32]:

$$0 = \sum_j F_{j \to i} C_j^{\alpha} + G_i^{\alpha} - \sum_j F_{i \to j} C_i^{\alpha} - R_i^{\alpha} \quad (11$$

C_i^{α} represents the contaminant air concentration as a mass ratio (mass of contaminant α in zone i/mass of air in zone i) and is reported as kg/kg. The first term in Equation 11 accounts for contaminant entry by inward flows ($F_{j \to i}$) through paths from nearby zone j to zone i. The third term indicates contaminant removal by outward airflows from zone i ($F_{i \to j}$).[32]

In this study, the contaminant is added or removed from a zone in a building by inward or outward airflows ($F_{j \to i}$ and $F_{i \to j}$), which are a function of wind and stack effect. Inward and outward air flows include air from outside the building as well as interzonal flows.

The second and last terms allow the contaminant to be added or removed from a zone at a constant generation (G_i^{α}) or removal (R_i^{α}) rates (kg/s of contaminant α). The COMSOL multiphysics program computes the mass entry rate and contaminant concentration near the foundation cracks solving a chemical transport equation which is coupled with a soil gas continuity equation. The resulting VI entry rate corresponds to G_i^{α} in equation 11. Although not included in this study, CONTAM includes R_i^{α}, which allows removal of the chemical from a zone at a given rate.

The general approach, for computing mass entry rate, has been well described previously[3]. COMSOL uses weak constraints to obtain accurate estimates of soil gas entry rates through the crack; and, then mass flux, a combination of advective and diffusive flux, into the building is calculated assuming 1D transport through the crack. Unlike previous studies, the COMSOL Multiphysics software is used to investigate the influence of wind/stack effects in both atmospheric and subsurface domains. In the current model application, Darcy's law

equation is coupled with RANS equations with turbulence models (k-ε) to solve turbulent wind flow above and around a building to obtain the mass entry rate by considering both wind and stack effects. The application of this model can be expanded to include contaminant mass entry through other entry points besides foundation cracks (i.e. preferential pathways). The mass entry rates from other sources would be combined with the mass entry rate determined for vapor intrusion (via cracks) by COMSOL and added to CONTAM as G_i^{α}.

COMSOL Multiphysics

Simulations in this study are carried out on a residential single story building with basement that extends 2m below ground surface (bgs). The air and soil domain dimensions are 200 m (Length) ×200 m (Width) ×50 m (Height) and 200 m (Length) ×200 m (Width) ×8 m (Height), respectively. The single-story building has a 10m×10m area with 3 m (Height) walls aboveground. The building has a roof that has an additional height of 1.8 m (≃20° slope) making the total building height 4.8 m above grade (Figure 2). The building is located in the center of soil and air domains. A perimeter crack with 0.005 m width and 0.1999 m^2 area is located around the basement foundation and serves as the entry point for contaminant vapors. All simulations are modeled for steady state conditions.

It is assumed that the subsurface domain consists of homogeneous soil. The source of the contaminant is assumed to be trichloroethylene (TCE) (MW=131.4 g/mol) located at 8 m bgs along the bottom of the entire modeling domain. The vapor source concentration is defined as 2.014×10^{-3} mol/m^3 which is consistent with the source concentration used in previous modeling studies[3] This concentration was selected for ease of comparison between previous and current studies. The total soil porosity and soil permeability to soil gas flow are 0.35 (m^3 voids)/(m^3 soil) and 1×10^{-12} m^2, respectively. The overall effective diffusion coefficient for transport in the porous media is 8.68×10^{-7} m^2/s in models. The diffusivity of TCE in air is equal to 7.4×10^{-6} m^2/s. In addition, one scenario with 10^{-14} m^2 soil permeability and 0.45 (m^3 voids)/(m^3 soil) total soil porosity is studied to investigate the influence of soil permeability and soil gas diffusion coefficient on contaminant concentration distribution in soil while wind blows above ground. The overall effective diffusion coefficient for transport in the porous media equals to 4.37×10^{-7} m^2/s in the latter scenario, which is consistent with the soil properties used in previous modeling studies.[3]

The element shape was tetrahedral. The minimum element size is 0.1 mm and the maximum element size is 2 m. The element growth rate is 1.5. The number of elements for the no wind flow scenario is 4.3519 $x10^6$ elements. The number of elements for scenarios with wind flow is $1.0086x10^7$ elements. All scenarios were run using the University of Kentucky high performance computing cluster (DLX2/3), which is a traditional batch-processing institutional cluster, with high-speed interconnects and a shared filesystem. The DLX cluster provides over 4800 processor cores, 18TB of RAM, and 1PB of high-speed disk storage. Model run times for scenarios with wind flow typically ranged from 1 to 4 hours.

CONTAM coupled with CFD0

This study is not meant to be representative of an actual building but to present a VI model that couples a multizone and CFD programs and is capable of generating soil vapor entry rates, indoor pressures, AERs and indoor concentrations in the presence of wind and stack effects. In the multizone model, all zones are assumed as well-mixed zones, which means each zone has been considered as a single node wherein air has uniform temperature, pressure and contaminant concentration. The building modeled in this study has two zones, the basement and the first floor which are connected by a stairway. The cross-sectional area of the stairs is equal to 10 m^2 and the stair treads are assumed to be closed. All simulations are modeled for steady state conditions.

The building is connected to outdoor area by a door in south and one window on each north and south sides of the building. There is no window or door on the east and west side of the building. Windows and doors are assumed to be closed and the only pathways through the building are the leakage areas in windows, doors and external walls. The plan view of the 1st floor and profile view of the building is shown in Figure 2.

In the present study, airflow through various pathways is modeled using powerlaw relationship (described in Model Method section). Perimeter cracks (5mm wide) allow soil gas to enter the building. The leakage characteristics for external walls, windows and doors can be gained based on range of leakage values for various components in chapter 26 of ASHRAE Handbook of Fundamentals, 2001.[34] The values of leakage areas used in this study are shown in Table 1 which are the best estimate values of leakage ranges suggested by ASHRAE Handbook of Fundamentals, 2001.[34] All leakage areas are based on a reference pressure (P_r) of 4 Pa and a discharge coefficient (C_d) of 1.0. Indoor air temperature in models is equal to 23°C which is a value inside the comfort zone (see Chapter 9, Figure 5 of ASHRAE[31]). Using Lexington, Kentucky as a representative case and considering 99.6% confidence, the maximum and minimum outdoor air temperatures are assumed to be 33°C and −12°C, respectively (see Chapter 9 of ASHRAE[31]).

Atmospheric boundary layer thickness (δ_{met}) and the exponent at meteorological station (α_{met}) are equal to 270m and 0.14, respectively (see Table 1, Chapter 24 of ASHRAE[31]). Assuming that the building is located in an urban and suburban location, δ and α values in equation 8 are equal to 370 m and 0.22, respectively. The CFD0 models simulate the wind flow with a range of 0° to 360° for wind direction with 15° increment. Wind flow above and around a building can affect the pressure distribution on the ground surface and under surface around the building. Figure 3 shows the daily wind speed fluctuations in Lexington, KY, in 2014 year (minimum and maximum wind speed are 0.9 to 9.4 m/s, respectively). Using Lexington as a representative case, we investigate the influence of wind speeds in the range of 1–10 m/s on atmospheric, subsurface and indoor air pressure, concentration of contaminant in the subsurface, AER and indoor air concentration.

Ventilation (natural and mechanical) is another important factor that affects indoor air pressure and contaminant concentrations in the building. However, these effects, are not included explicitly in the application of this model. Inclusion of ventilation in VI modeling is a topic of ongoing and future research. The AER values calculated in this study are

specific for the conditions modeled and are fairly low when considered in the context of typical US residential AER values, which often include the contribution of ventilation.[22]

RESULTS AND DISCUSSION

The sections below present several scenarios to highlight key aspects of this modeling approach. A simplified building was used to illustrate the model, therefore the results are not meant to necessarily represent a particular "real-world" building. As the subsequent sections will highlight, a key advantage of the modeling approach presented here, is that it can capture the influence of weather conditions and building features when calculating indoor air concentrations. Many previous VI models[e.g. 2, 3] apply a user-defined AER value of 0.5 1/hr. However, for the building modeled herein with few features prone to leakage (e.g. concrete external walls, 2 windows and a door), the resulting AER is appropriately low for the no wind scenario (0.06 1/hr). A building with different characteristics and different weather conditions, a different AER would be expected. Reichman et al.[22] discuss the variability of AERs in US residential buildings and highlight factors that influence building-specific AERs. The modeling approach presented here directly estimates an AER that is representative of the building and weather (e.g. wind and stack effects) and provides a more informed estimate of the VI exposure risk.

Indoor air pressure and AER

This study investigates how wind speed (WS) (0, 1m/s, 5m/s and 10 m/s), wind direction (WD) (0° to 360° with 15° increment), temperature difference (i.e. stack effect) between outdoor and indoor ($\Delta T = T_{out} - T_{in}$) equal to +10°C (33°C-23°C), 0°C (23°C-23°C), −15°C (8°C–23°C) and −35°C (−12°C–23°C) and building characteristics (window and door layout) affect indoor pressure and corresponding AER. Figure 4(a) shows the effect of the above-mentioned parameters on AER values for all the scenarios.

To investigate the influence of stack effect, different ΔT values were defined, while maintaining WS=0. For the scenario with no wind speed (WS= 0 m/s) and ΔT= 0°C, the AER value is equal to 0 (see Figure 4(a) green line with x symbols). The results show increasing trend for AER as the absolute value of ΔT increases. Consequently, the scenario with the largest temperature difference (ΔT= −35°C) resulted the highest AER value among the scenarios, regardless of wind speed (see Figure 4(a) blue line--all symbols).

Wind speed is another factor that can influence AER value in a building. The results indicate that when wind speed increases, the building AER value increases. In addition, wind direction can influences AER values, especially for a 10 m/s wind speed. As shown in Figure 2a, north side (0 to 45° and 315° to 360° wind direction) and south side (135° to 225° wind direction) of the building are leakier than the east and west walls (45° to 135° and 225° to 315° wind directions, respectively). 90° and 270° wind directions blow perpendicularly on the tight side of building. For a constant wind speed, AER reaches the highest values when wind blows on the leakier (north and south) side of the building and lowest values when wind blows on the tighter (east and west) side of the building. Figure 4a shows that stack effect is typically small compared to wind effect in changing AER values for the conditions modeled here.

Figure 4b shows the influence of wind speed, wind direction and stack effect on basement pressure. The horizontal lines show the influence of stack effect (WS ≤ 1 m/s). When WS ≤ 1 m/s and ΔT is equal to zero, the basement pressure is near to zero. For scenarios with WS ≤ 1 m/s (horizontal lines) and when outdoor temperature is less than indoor temperature (ΔT= −15°C and ΔT= −35°C), the basement is under-pressurized; however when outdoor temperature is higher than indoor temperature (ΔT= +10°C) the basement is over-pressurized.

For WS≥ 5m/s, the basement is over-pressurized when wind blows on the leaky side of the building, but the basement is under-pressurized when wind blows on the tight side of the building. These results are for the specific building modeled; however they emphasize that wind direction and opening locations play an important role in estimating basement pressure. Depending on wind direction and opening location, a building can be under-pressurized or over-pressurized at the same wind speeds and ΔT values. Other wind speeds may also be of interest; however the overall effect will depend on building features, wind directions and temperature differences.

Pressure and concentration profiles

COMSOL Multiphysics program is used to couple the outdoor atmospheric air and soil domains to investigate the influence of wind flow above- and below ground. Two different scenarios were defined to study the wind effect (WS=10 m/s and 0 m/s). Both scenarios were modeled for ΔT = −35°C. Soil properties in both scenarios are 0.35 (m^3 voids)/(m^3 soil) total soil porosity and 1×10^{-12} m^2 soil permeability. The overall effective diffusion coefficient for transport in the porous media is 8.68×10^{-7} m^2/s in both scenarios. Figure 5(a1) shows the pressure profile when WS=10 m/s. The wind flow produces an asymmetric pressure profile in both air and soil domains. The pressure is higher on the windward side and lower on the leeward side.

The plan view of the pressure profiles indicates that the lowest pressure happens on the lateral sides of the building (Figure 5(a-1)). The pressure reaches +30 Pa on the windward side and −45 Pa on the lateral sides of the building. This pressure gradient around building influences the pressure difference between indoor and outdoor, which is an important feature that was not previously identified by VI models.[18, 20]

Figure 5(a-2) shows the pressure profile for WS=0 m/s, which is the same scenario that has been most commonly modeled by previous VI models.[20] The pressure profile is symmetric and basement air pressure is determined (due to stack effect only) to be −5.2 Pa for ΔT= −35°C.

Figure 5b shows the concentration profiles for the same scenarios (WS=10 m/s and 0 m/s, ΔT= −35°C). The concentration profile is symmetric when WS=0 m/s; however for WS=10 m/s, the concentration profile is slightly asymmetric (Figure 5(b-2)). To investigate the influence of wind on soil gas concentrations in a less permeable soil (10^{-14} m^2 soil permeability, see COMSOL Multiphysics section). The results indicate that for this case, wind does not have an effect on contaminant concentration distribution for WS ≤ 10 m/s. Therefore, the influence of wind is most likely important due to the role it plays on pressure

profiles, and for soil gas concentrations for high permeability soils or possibly when wind speeds are high (>10m/s).

Indoor air concentration

Table 2 and Figure 6 summarize the results of twelve (12) different modeled scenarios. The influence of ΔT, WD, and WS are considered with respect to AER, contaminant mass entry rate and indoor concentration.

Figure 6a show that mass entry rate of the contaminant through the foundation crack is inversely related to the basement pressure for all scenarios. In addition, scenarios with low (negative) basement pressures and high mass entry rates have higher C_C/C_S values (Table 2). As with other previous modeling efforts, a decrease in basement pressure causes the contaminant to enter the basement at a higher rate. Air flow due to contaminant entry/exit through the crack and wind flow around the building can dilute contaminant concentrations near the foundation. The basement pressure for all scenarios modeled here (Figure 6a and Table 2) is obtained by coupling indoor and outdoor domains, rather than a user defining a specific basement pressure.

Scenario 11 (ΔT=0, WD=0, WS=10 m/s) is the most over pressurized scenario and has the lowest mass entry rate (among the scenarios modeled). In this scenario, wind blows on the leaky side of the building and outdoor temperature is higher than the indoor temperature, which results in a higher basement pressure than other scenarios. The external (asymmetric) pressure profile around the building caused by wind can still result in a pressure differential between the outdoor and indoor domains that allows soil gas to enter the building; however it results in the lowest VI exposure risks due to the relatively high basement pressure, as well as a high AER value. The highest AER values were obtained for scenarios when WD=0 (wind was blowing on the leaky side of the building) and WS=10 m/s. The results show that when WS=0 (stack effect only), the AER values are the lowest among all of the scenarios modeled.

Figure 6b and 6c shows the relationship between AER and C_{FF}/C_S and C_B/C_S. The results show AER appears to be a dominant factor in controlling C_{FF}; however, AER is not the dominant factor that controls C_B. This VI modeling approach uses a multizone model to calculate indoor air concentrations in different zones. In this model, no windows were included in the basement zone; however a stairway connected the first floor to basement and allowed air flow between the first floor and basement. AER is not the dominant factor that controls the indoor air concentration in the basement. Other factors such as basement pressure and mass entry rate of contaminant through the cracks directly influence the basement air concentration.

The AER reported in Table 2 is calculated as a value for the entire house. Since the first floor has more openings, the AER value is more representative of the first floor, than it is of the basement. However, C_B is calculated based on the mass balance equations (see Model Method section), which is considerably different than previous VI modeling approaches. Here, indoor air concentrations are determined for different zones based on the air flow characteristics of specific zones.

Special considerations and limitations

The following subsections discuss several special considerations and limitations of the current modeling approach. Table 3 summarizes comparisons between previous modeling approaches[2,3] and the current model, as well as the special consideration of paving around a building.

Comparison with Previous Modeling Studies—The model results for specific scenarios (no wind) were compared to two previously published 3D VI models.[2, 3] It is only possible to compare the current modeling approach no wind (WS=0) scenarios because the previous models did not include wind flow. Abreu and Johnson[2] and Pennell et al.[3] set user-defined values for ΔP=5Pa (under-pressurized inside the building) and AER (0.5 1/hr); however they used different computational methods, finite difference and finite element, respectively. In the current modeling study, the indoor air pressure, outdoor air pressure, and AER are calculated directly by the model.

The results summarized in Table 3 for Abreu and Johnson[2], Pennell et al.[3] and the current study agree well. Pennell et al.[3] modeled a characteristic entrance region (CER) as 10cm and then assumed all soil gas flowed through the 5 mm crack (due to continuity). Given steep pressure and soil gas concentration gradients in the region of the CER, differences in the soil gas flow rate and soil gas concentrations may be responsible for the reported difference in Table 3. The difference between the current study and Abreu and Johnson's[2] model results is likely due to the fact that the soil properties and the computational modeling approach was different (see Table 3 notes).

A building surrounded by 5m paved ground was investigated in Pennell et al[3]. For comparison purposes, this special case was also investigated using the current modeling approach. For no wind (WS=0) and paved ground, the soil gas flow rate is 0.38 L/min in Pennell et al.[3] and 0.32 L/min in this study match well, especially given the difference in modeling approaches (e.g. CER vs crack). The results indicate that the soil gas flow rate decreases when a paved surface is present around the building. The mass entry rate of contaminant through the foundation crack is 1.25 μg/s and 1.81 μg/s for unpaved and paved ground in Pennell et al.[3], respectively. In the current study, the mass entry rate for unpaved ground is 1.01 μg/s, compared to 1.56 μg/s for paved ground. While these mass flow rates in the current study are lower than the values reported in Pennell at al.[3], they follow a similar trend in which the paved ground has a higher mass entry rate. The reason for lower mass entry rates is likely due to the CER vs crack and mesh sizes in finite element study in Pennell et al.[3] compared to the current study.

Lastly, an important consideration for model comparison is the indoor air concentration divided by the source concentration (C_{in}/C_S). In Table 3, $C_{in}/C_{S.}$ values for Pennell et al.[3] and Abreu and Johnson[2] are provided as reported in the literature. These values are calculated using the approach described by Pennell et al.[3] and Abreu and Johnson[2],

where,

$$C_{in} = \frac{Mass\ entry\ rate}{AER \cdot Volume\ of\ enclosed\ space + Soil\ gas\ flow\ rate} \quad (12$$

The C_{in}/C_S values rely on user-defined AERs and do not incorporate the AERs that are estimated by the current modeling approach. Pennell et al.[3] and current study used an enclosed space value of 233 m^3 to calculate C_{in}/C_S. Abreu and Johnson[2] used 174 m^3 for the volume of the enclosed space and explains the difference in C_{in}/C_S values reported in Table 3.

Wind Effects and Paved Ground Surface—Two scenarios with 10 m/s wind speed and two different wind directions (0 and 90 degree) were modeled with and without 5m paved ground surface extending around the building. The scenario with WD=0 (leaky side of the building) is less under-pressurized with lower soil gas flow rate and mass entry rate compared to no wind flow scenario. The scenario with WD=90 (tight side of building) is more under-pressurized with higher values of soil gas flow rate and mass entry rate compared to the WD=0 scenario.

Wind flow can cause higher soil gas flow or lower soil gas flow for paved ground scenarios depending on the wind direction; however a paved ground around the building causes higher mass entry rates through the crack because the contaminant accumulates under the paved ground and building. Paved surfaces can also cause higher indoor air concentration for both basement and first floor space.

C_B/C_S and C_{FF}/C_S values are determined using CONTAM and rely on the current modeling approach described in Figure 1. Like the existing VI models, the paved surface has a higher indoor air concentration due to higher mass entry rates. However, the current modeling approach provides weather and building-specific indoor pressures and AER values, which directly influence the indoor air concentrations. The multi-zone indoor air modeling approach, provides different estimates for indoor air concentrations depending on location. For the building modeled, the data shows that the basement indoor air concentration is higher than the first floor, regardless of whether a paved surface is present around the building.

Comparison with Field Data—The model results in this study were qualitatively compared to field data collected by Lou et al..[4] Lou et al.[4] collected these field data beneath and around a slab-on-grade building overlying a petroleum hydrocarbon impacted soil in Evansville, WY. The field data indicated that dominant wind direction was southwest and the pressure difference (indoor and shallow soil) on the windward side of the building (south west side) was higher than the leeward side of the building (northeast side). They reported pressure differences in the range of 4.4–17 Pa on windward side for WS=5.1m/s. The model results in the current study show a similar trend to the field study (i.e. higher pressure difference in the windward side and lower pressure difference at the leeward side) in soil. The pressure difference in present study lies in the range of 3.6–10.9 Pa, which is in a good agreement with the field study by Lou et al.[4] They also showed that the contamiant and

oxygen concentration in soil depend on dominant wind direction in the area. Contamiant and oxygen concentartion were lower and higher, repectively, in the windward side of dominant wind direction. An opposite trend was observed at the leeward side which indicates the dominant wind direction is able to influence (through fate and transport processes) the contaminant distribution in soil due to the dominant wind direction.

Steady State Limitations of the Current Study—Additional model simulations were conducted to investigate timescales necessary to reach steady-state pressure profiles in aboveground and subsurface domains. The data (not shown) suggest that times are typically much shorter (e.g. minutes) for pressure profiles in the atmosphere and along the ground surface to reach steady state as compared to times for soil gas concentrations (e.g. days to months to years) to reach stead state in the subsurface. While the time to reach steady state is scenario specific and will depend on many different conditions, steady-state simulations provide useful information, even though wind flows may not be constant.

As discussed above, the results of the field study by Lou et al. [4] suggest that soil gas pressure and concentration of an aerobically degradable contaminant are influenced by dominant wind direction. Steady state modeling may be an important simplification to assist in better understanding VI exposure risks influenced by dominant wind flows. However, transient modeling may be important for AER and indoor pressure estimation and additional research is needed.

CONCLUSIONS

To date, most VI models have focused on subsurface fate and transport processes coupled with stack effects (i.e. user-defined ΔP); in this study we developed a comprehensive model that combines three different domains: the atmospheric domain (outdoor above-ground), indoor domain, and subsurface domain. The results suggest that wind flows can result in asymmetrical pressure profiles; and for permeable soils at moderate to high wind speed scenarios, soil gas concentrations may also exhibit asymmetric profiles.

Asymmetric pressure profiles around buildings can cause infiltration in the windward side and exfiltration on the leeward side of the building, which influences indoor air pressure and the mass entry rate of contaminant. Results show that the indoor air contaminant concentration is influenced by the AER which is a function of wind speed, wind direction and temperature difference. The results also indicate that when the wind speed increases and blows on the leaky side of the building, the indoor pressure and AER increase, which causes a decrease in the contaminant mass entry rate and indoor air concentration. When the wind speed increases and blows on the tight side of the building, the indoor air pressure and AER decreases and mass entry rate and indoor air concentration increases. The VI model presented here provides an improved conceptual understanding of how wind and stack effects influence VI exposure risks due to changes in AER, indoor/outdoor air pressures.

The results for the current modeling approach are for the special case of homogenous soils and steady state conditions. The influence of other factors that can affect VI exposure risks, such as heterogeneous soil in the subsurface, the presence of preferential pathways, and

variable soil moisture have not been investigated in this study. However, the modeling approach presented can be used to consider the influence of these effects.

Supplementary Material

Refer to Web version on PubMed Central for supplementary material.

Acknowledgments

The project described was supported by University of Kentucky Superfund Research Program from the National Institute of Environmental Health Sciences [Grant Number P42ES007380] and by the National Science Foundation [Grant Number 1452800]. The content is solely the responsibility of the authors and does not necessarily represent the official views of the National Institute of Environmental Health Sciences, the National Institutes of Health or the National Science Foundation.

References

1. U.S. Environmental Protection Agency. OSWER technical guide for assessing and mitigating the vapor intrusion pathway from subsurface vapor sources to indoor air. Environmental Protection Agency; Washington, DC: 2015. https://www.epa.gov/sites/production/files/2015-09/documents/oswer-vapor-intrusion-technical-guide-final.pdf [accessed September 2017]
2. Abreu LDV, Johnson PC. Effect of Vapor Source–Building Separation and Building Construction on Soil Vapor Intrusion as Studied with a Three-Dimensional Numerical Model. Environ Sci Technol. 2005; 39:4550–4561. DOI: 10.1021/es049781k [PubMed: 16047792]
3. Pennell KG, Bozkurt O, Suuberg EM. Development and application of a three-dimensional finite element vapor intrusion model. J Air Waste Manage Assoc. 2009; 59:447–460. DOI: 10.3155/1047-3289.59.4.447
4. Luo H, Dahlen P, Johnson PC, Peargin T, Creamer T. Spatial Variability of Soil-Gas Concentrations near and beneath a Building Overlying Shallow Petroleum Hydrocarbon–Impacted Soils. Groundwater Monit Rem. 2009; 29:81–91. DOI: 10.1111/j.1745-6592.2008.01217.x
5. Abreu LDV, Johnson PC. Simulating the Effect of Aerobic Biodegradation on Soil Vapor Intrusion into Buildings: Influence of Degradation Rate, Source Concentration and Depth. Environ Sci Technol. 2006; 40:2304–2315. DOI: 10.1021/es051335p [PubMed: 16646467]
6. Bozkurt O, Pennell KG, Suuberg EM. Simulation of the Vapor Intrusion Process for Nonhomogeneous Soils Using a Three-Dimensional Numerical Model. Groundwater Monit Rem. 2009; 29:92–104. DOI: 10.1111/j.1745-6592.2008.01218.x
7. Abreu, LDV. PhD thesis. Arizona State University; 2005. A Transient Three Dimensional Numerical Model to Simulate Vapor Intrusion Into Buildings.
8. Diallo TM, Collignan B, Allard F. 2D Semi-empirical models for predicting the entry of soil gas pollutants into buildings. Building and Environment. 2015; 85:1–16. DOI: 10.1016/j.buildenv.2014.11.013
9. Diallo TMO, Collignan B, Allard F. Analytical quantification of airflows from soil through building substructures. Building Simulation. 2013; 6:81–94. DOI: 10.1007/s12273-012-0095-2
10. U.S. Environmental Protection Agency. User's guide for evaluating subsurface vapor intrusion into buildings. Environmental Protection Agency; Washington, DC: 2004. EPA-68-W-02-33http://www.dtsc.ca.gov/AssessingRisk/upload/VI_USEPA_Users-guide.pdf [accessed September 2017]
11. Johnson PC, Ettinger RA. Heuristic model for predicting the intrusion rate of contaminant vapors into buildings. Environ Sci Technol. 1991; 25:1445–1452. DOI: 10.1021/es00020a013
12. Luo, H. PhD thesis. Arizona State University; 2009. Field and modeling studies of soil vapor migration into buildings at petroleum hydrocarbon impacted sites.
13. Pennell KG, Scammell MK, McClean MD, Suuberg EM, Moradi A, Roghani M, Ames J, Friguglietti L, Indeglia PA, Shen R, Yao Y, Heiger-Bernays WJ. Field data and numerical modeling: A multiple lines of evidence approach for assessing vapor intrusion exposure risks. Sci Total Environ. 2016; 556:291–301. DOI: 10.1016/j.scitotenv.2016.02.185 [PubMed: 26977535]

14. Riley W, Gadgil A, Bonnefous Y, Nazaroff W. The effect of steady winds on radon-222 entry from soil into houses. Atmos Environ. 1996; 30:1167–1176. DOI: 10.1016/1352-2310(95)00248-0
15. Riley WJ, Robinson AL, Gadgil AJ, Nazaroff WW. Effects of variable wind speed and direction on radon transport from soil into buildings: model development and exploratory results. Atmos Environ. 1999; 33:2157–2168. DOI: 10.1016/S1352-2310(98)00374-4
16. Shen R, Pennell KG, Suuberg EM. A numerical investigation of vapor intrusion—The dynamic response of contaminant vapors to rainfall events. Sci Total Environ. 2012; 437:110–120. DOI: 10.1016/j.scitotenv.2012.07.054 [PubMed: 22922135]
17. Shen R, Pennell KG, Suuberg EM. Analytical modeling of the subsurface volatile organic vapor concentration in vapor intrusion. Chemosphere. 2014; 95:140–149. DOI: 10.1016/j.chemosphere.2013.08.051 [PubMed: 24034829]
18. Shen R, Suuberg EM. Impacts of changes of indoor air pressure and air exchange rate in vapor intrusion scenarios. Building and Environment. 2016; 96:178–187. DOI: 10.1016/j.buildenv.2015.11.015 [PubMed: 28090133]
19. Song S, Schnorr BA, Ramacciotti FC. Quantifying the Influence of Stack and Wind Effects on Vapor Intrusion. Human and Ecological Risk Assessment: An International Journal. 2014; 20:1345–1358. DOI: https://doi.org/10.1080/10807039.2013.858530.
20. Yao Y, Shen R, Pennell KG, Suuberg EM. A Review of Vapor Intrusion Models. Environ Sci Technol. 2013; 47:2457–2470. DOI: 10.1021/es302714g [PubMed: 23360069]
21. U.S. Environmental Protection Agency. Vapor Intrusion Screening Level (VISL) Calculator User Guid. Environmental Protection Agency, Office of Solid Waste and Emergency Response (OSWER) and Office of Superfund Remediation and Technology Innovation (OSTRI); Washington, DC: May. 2014 https://www.epa.gov/sites/production/files/2015-09/documents/visl-usersguide_1.pdf [accessed September 2017]
22. Reichman R, Shirazi E, Colliver DG, Pennell KG. US residential building air exchange rates: new perspectives to improve decision making at vapor intrusion sites. Environ Sci: Processes Impacts. 2017; 19:87–100. DOI: 10.1039/C6EM00504G
23. Dols WS. A tool for modeling airflow & contaminant transport. ASHRAE J. 2001; 43:35.
24. Feustel HE, Dieris J. A survey of airflow models for multizone structures. Energy and Buildings. 1992; 18:79–100. DOI: https://doi.org/10.1016/0378-7788(92)90040-N.
25. Haghighat F, Li H. Building airflow movement — validation of three airflow models. Journal of Architectural and Planning Research. 2004; 21:331–349.
26. Wang H, Zhai ZJ. Advances in building simulation and computational techniques: A review between 1987 and 2014. Energy and Buildings. 2016; 128:319–335. DOI: 10.1016/j.enbuild.2016.06.080
27. Persily, AK. Modeling radon transport in multistory residential buildings, ASTM STP 1205. Nagda, Niren L., editor. American Society for Testing and Materials; Philadelphia: 1993. p. 226-242.
28. Wang, L. PhD thesis. Purdue University; 2007. Coupling of multizone and CFD programs for building airflow and contaminant transport simulations.
29. Wang LL, Dols WS, Chen Q. Using CFD capabilities of CONTAM 3.0 for simulating airflow and contaminant transport in and around buildings. HVACR Res. 2010; 16:749–763.
30. Sherman, M. Simplified modeling for infiltration and radon entry. Proceedings, Thermal Performance of the Exterior Envelopes of Buildings Conference V; 1992;
31. American Society of Heating, Refrigerating and Air-Conditioning Engineers (ASHRAE). 2013 ASHRAE Handbook-Fundamentals. ASHRAE; Atlanta, GA: 2013.
32. Dols, WS., Polidoro, BJ. CONTAM User Guide and Program Documentation: Version 3.2. National Institute of Standards and Technology; 2015. http://dx.doi.org/10.6028/NIST.TN.1887 [accessed September 2017]
33. Orme, M., Liddament, MW., Wilson, A. An analysis and data summary of the AIVC's numerical database. Oscar Faber; 1994.
34. American Society of Heating, Refrigerating and Air-Conditioning Engineers (ASHRAE). 2001 ASHRAE Handbook-Fundamentals. ASHRAE; Atlanta, GA: 2001.

35. Holmes, J. Wind loads on low-rise buildings: The structural and environmental effects of wind on buildings and structures, Chapter 12, Faculty of Engineering. Monash University; Melbourne, Australia: 1986.

36. Holmes JD. Wind pressures on tropical housing. Journal of Wind Engineering and Industrial Aerodynamics. 1994; 53:105–123. DOI: https://doi.org/10.1016/0167-6105(94)90021-3.

37. Weather Underground. [accessed September 2017] http://www.wunderground.com/history/airport/KLEX/2014/1/14/DailyHistory.html

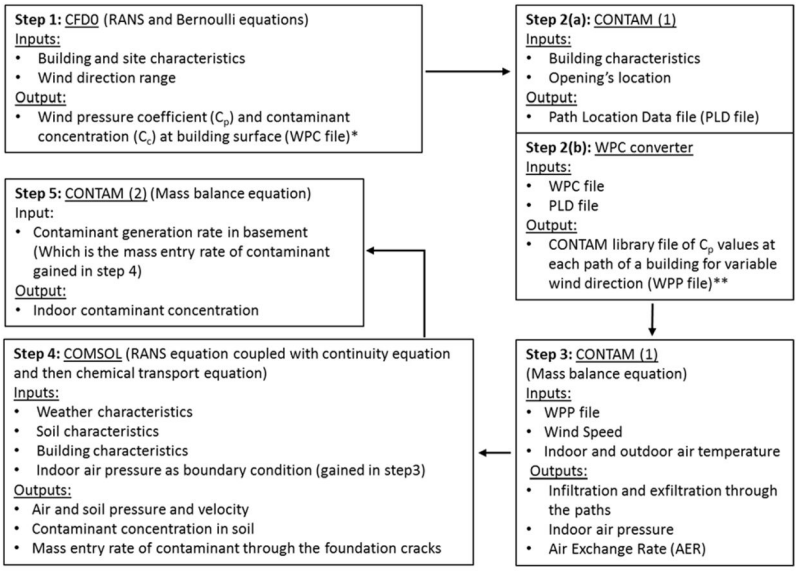

Figure 1.

Overview of modeling process

*(1) In the present study, there is no external contaminant source, so the C_c values in WPC file are equal to zero

*(2) WPC file for each path contains building envelope C_p values for all assigned wind directions

**WPP file: Wind Pressure Profile

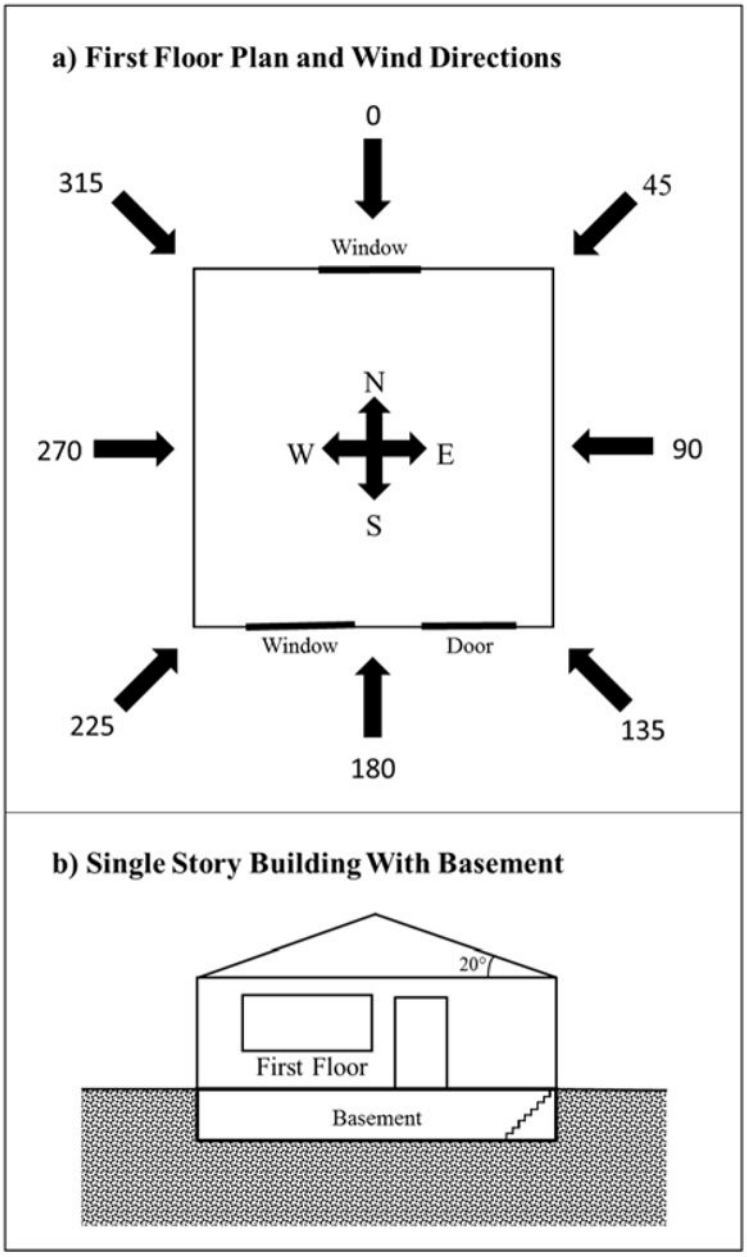

Figure 2.
a) 1st floor plan view and wind directions blew on building b) elevation of the modeled building

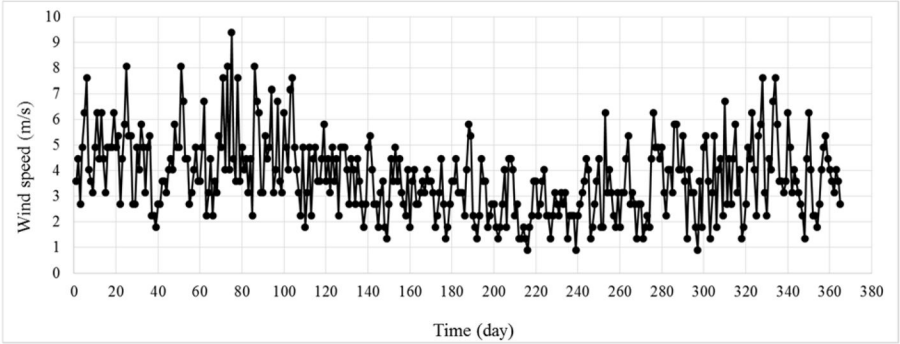

Figure 3.

Average daily wind speed in Lexington, KY (1 Jan–31 Dec, 2014). Weather Underground (Accessed September 2017)[37]

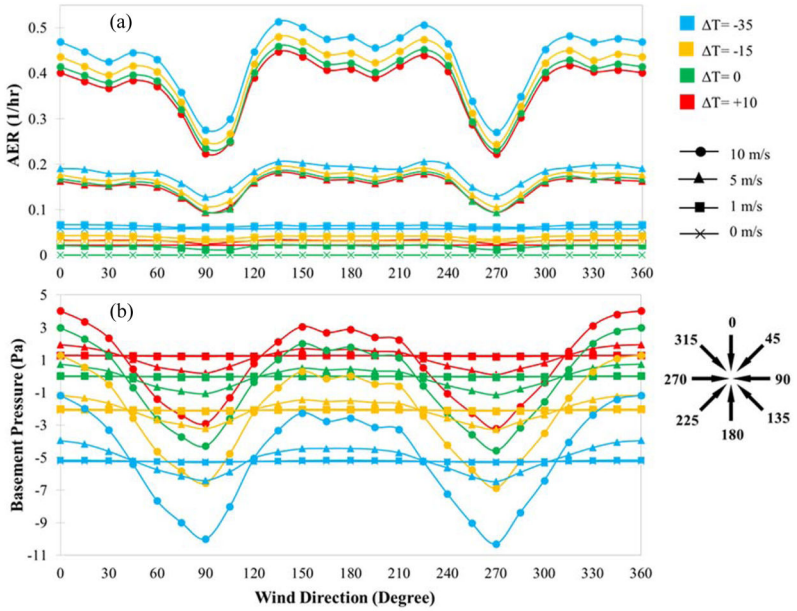

Figure 4.
Wind and Stack Effect on Building AER (a) and Basement Pressure (b)

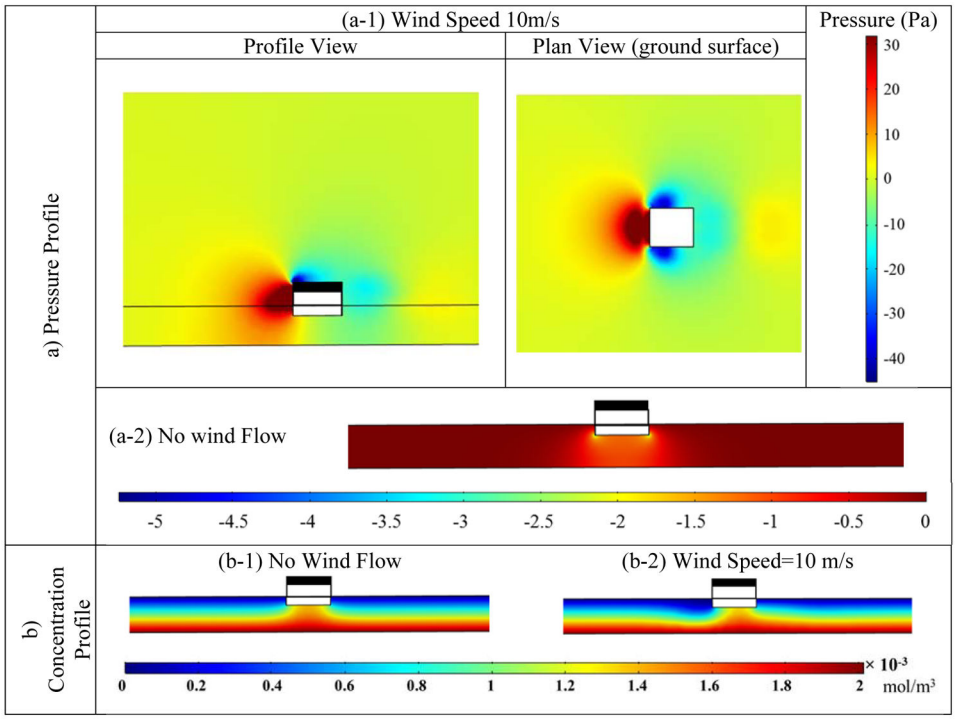

Figure 5.

a) Pressure profile in air and soil domains, with 10 m/s wind flow (a-1) and without wind flow (a-2), b) Normalized concentration profile in air and soil, without wind flow (b-1) and with 10 m/s wind flow (b-2)

*Figures are cropped to show area around building to save space.

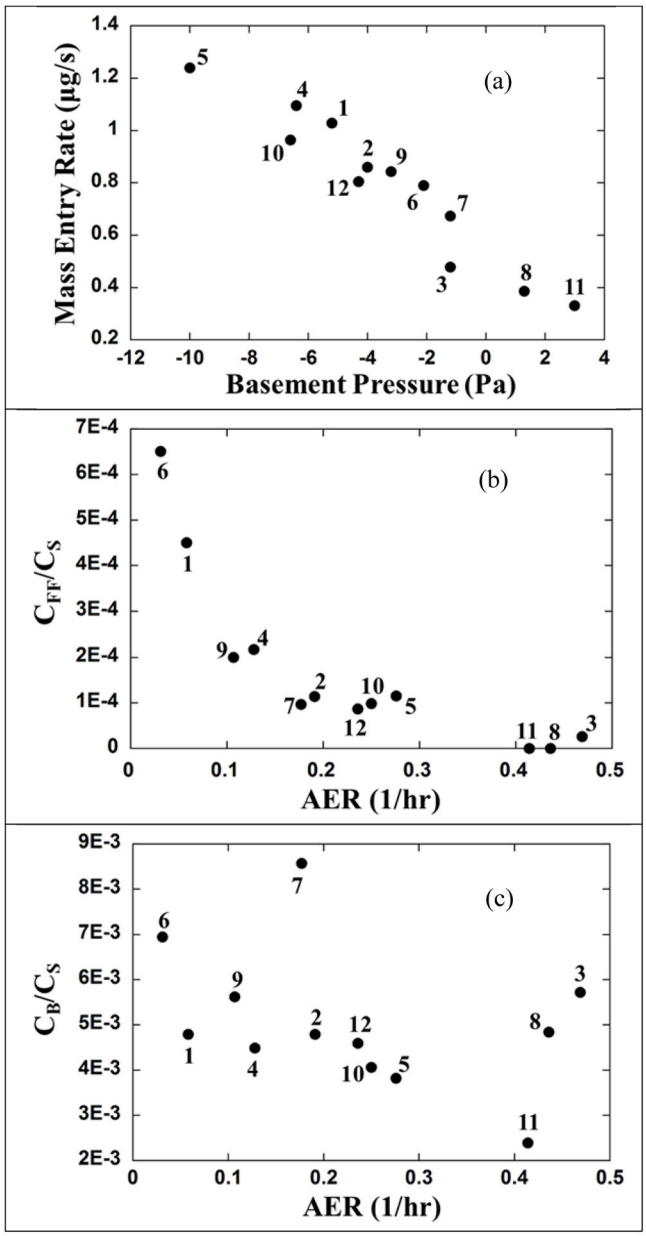

Figure 6.

a) The mass entry rate of contaminant through the crack vs. basement pressure, b) Normalized contaminant concentration in first floor vs. AER and c) Normalized contaminant concentration in basement vs. AER

Table 1

Effective air leakage areas used in this study (best estimate values in ASHRAE, 2001[34])

Path	Type	Units	Best Estimate
Door frame	General	cm^2/ea	12
Door	Single, not weather-stripped	cm^2/ea	21
Exterior walls	Precast concrete panel	cm^2/m^2	1.2
Window framing	Masonry, uncaulked	cm^2/m^2	6.5
Windows	Awning, not weather-stripped	cm^2/m^2	1.6

Table 2

Summary of Model Results

Scenario #	Scenario WD-WS-(ΔT)	Basement Pressure (Pa)	Flow Direction	AER (1/hr)	Mass entry rate (μg/s)	C_C/C_S^*	C_B/C_S^*	C_{FF}/C_S^*
1	N/A-0-(−35)	−5.2	B to FF	0.06	1.03	0.289	4.79E-3	4.50E-4
2	0-5-(−35)	−4.0	B to FF	0.19	0.86	0.276	4.79E-3	1.14E-4
3	0-10-(−35)	−1.2	B to FF	0.47	0.48	0.220	5.72E-3	2.60E-5
4	90-5-(−35)	−6.4	B to FF	0.13	1.10	0.294	4.49E-3	2.17E-4
5	90-10-(−35)	−10.0	B to FF	0.28	1.24	0.290	3.82E-3	1.15E-4
6	N/A-0-(−15)	−2.1	B to FF	0.03	0.79	0.268	6.94E-3	6.51E-4
7	0-5-(−15)	−1.2	B to FF	0.18	0.67	0.257	8.57E-3	9.68E-5
8	0-10-(−15)	+1.3	FF to B	0.44	0.39	0.209	4.84E-3	0
9	90-5-(−15)	−3.2	B to FF	0.11	0.84	0.273	5.62E-3	2.00E-4
10	90-10-(−15)	−6.6	B to FF	0.25	0.96	0.272	4.06E-3	9.82E-5
11	0-10-(0)	+3.0	FF to B	0.41	0.33	0.200	2.39E-3	0
12	90-10-(0)	−4.3	B to FF	0.24	0.81	0.260	4.59E-3	8.70E-5

*C_C: Foundation crack TCE concentration, C_B: TCE concentration in basement indoor air, C_{FF}: TCE concentration in first floor indoor air and C_S: TCE (vapor) concentration of source (modeled as 2.014×10^{-3} mol/m^3 (See COMSOL Multiphysics Section))

Table 3

Comparison of Model Results for Select Cases

	Scenario WD-WS-(ΔT)	Paved	Basement Pressure (Pa)	AER (1/hr)	Soil gas flow (L/min)	Mass entry rate (μg/s)	C_{in}/C_S	C_B/C_S New approach	C_{FF}/C_S New approach
Abreu and Johnson[2]	No Wind	N	−5 user defined	0.5 user defined	0.40	NR	2.22E-4	NA	NA
Pennell et al.[3]	No Wind	N	−5 user defined	0.5 user defined	0.47	1.25	1.46E-4	NA	NA
		Y			0.38	1.81	2.11E-4	NA	NA
Current Study	No Wind	N	−5 user defined	0.5 user defined	0.38	1.01	1.18E-4	NA	NA
		Y			0.32	1.56	1.82E-4	NA	NA
	0-10-(−35)	N	−1.2 model result	0.47 model result	0.19	0.48	NA	5.72E-3	2.60E-5
		Y			0.03	1.07	NA	1.28E-2	5.82E-5
	90-10-(−35)	N	−10 model result	0.28 model result	0.65	1.24	NA	3.82E-3	1.15E-4
		Y			0.67	2.16	NA	6.67E-3	2.00E-4

Notes: NR- Not Reported. NA – Not Applicable. Values for Abreu and Johnson[2] and Pennell et al.[3] are provided as reported in the literature. Paving around the building includes 5m of impervious surface around the entire building (as described by Pennell et al.[3] Current Study “No wind” scenario was modeled to approximate the previous modeling approach by Abreu and Johnson[2] and Pennell et al.[3] The current study and Pennell et al[3] used the same soil gas effective diffusivity, air diffusivity and vapor source concentrations. Abreu and Johnson[2] used different values for the diffusivity in soil (1.036×10^{-6} m^2/s), air diffusivity (8.8056×10^{-6} m^2/s) and the vapor source concentration (200 mg/L).